Tail gut endoderm and gut/genitourinary/tail development: a new tissue-specific role for Hoxa13.

Pascal de Santa Barbara, Drucilla J. Roberts

▶ **To cite this version:**

Pascal de Santa Barbara, Drucilla J. Roberts. Tail gut endoderm and gut/genitourinary/tail development: a new tissue-specific role for Hoxa13.. Development (Cambridge, England), 2002, 129 (3), pp.551-61. inserm-00287639

HAL Id: inserm-00287639

https://www.hal.inserm.fr/inserm-00287639

Submitted on 12 Jun 2008

HAL is a multi-disciplinary open access archive for the deposit and dissemination of scientific research documents, whether they are published or not. The documents may come from teaching and research institutions in France or abroad, or from public or private research centers.

L'archive ouverte pluridisciplinaire **HAL**, est destinée au dépôt et à la diffusion de documents scientifiques de niveau recherche, publiés ou non, émanant des établissements d'enseignement et de recherche français ou étrangers, des laboratoires publics ou privés.

TAIL GUT ENDODERM AND GUT/GENITOURINARY/TAIL DEVELOPMENT: A NEW TISSUE SPECIFIC ROLE FOR *HOXA13*

Pascal de Santa Barbara and Drucilla J. Roberts

Harvard Medical School

Massachusetts General Hospital

Departments of Pathology and Pediatric Surgery Research

Fruit Street

Boston, MA 02114

Correspondence should be addressed to D.J.R. (email: robertsd@helix.mgh.harvard.edu)

Short title: Endodermal role for *Hoxa13*

Key words: *Hoxa13*, tail, endoderm, gut, HFG, development

SUMMARY *Hoxa13* is expressed early in the caudal mesoderm and endoderm of the developing hindgut. The tissue specific roles of *Hoxa13* function have not been described. Hand-Foot-Genital syndrome, a rare dominantly inherited human malformation syndrome characterized by distal extremity and genitourinary anomalies, is caused by mutations in the *Hoxa13* gene (*HFGa13*). We show evidence that one specific HFGa13 mutation likely acts as a dominant negative *in vivo*. When chick *HFGa13* is overexpressed in the chick's caudal endoderm early in development, caudal structural malformations occur. The phenotype is specific to *HFGa13* expression in the posterior endoderm and includes taillessness and severe gut/genitounrinary (GGU) malformations. Finally, we show that chick HFGa13 negatively regulates expression of *Hoxd13* and antagonizes functions of both endogenous Hoxa13 and Hoxd13 proteins. We suggest a fundamental role for epithelial specific expression of *Hoxa13* in the epithelial-mesenchymal interaction necessary for tail growth and posterior GGU patterning.

INTRODUCTION

Vertebrate gastrulation events form the three germ layers and pattern the early anterior body region. Although disputed, the posterior region likely forms via a separate secondary event at the undifferentiated mesenchyme of the tailbud to form the tail somites, distal neural tube, notochord, and tailgut (Catala et al., 1995; Gajovic et al., 1993; Griffith et al., 1992; Holmdahl, 1925; Knezevic et al., 1998; Pasteels, 1943; Schoenwolf, 1977; Schoenwolf, 1979). A critical early event in patterning the posterior embryo is the formation of the caudal intestinal portal (CIP), which initiates the development of the hindgut, tail, and forms the cloaca (the common gut/genitourinary (GGU) chamber). The cloaca is maintained throughout life in avian and some other vertebrate species. In mammals, the cloaca exists as an embryologic structure that undergoes septation to become distinct urethral, anal, and genital orifices. Abnormal development of the cloaca causes severe congenital malformations in vertebrates including humans (Kluth et al., 1995; Martinez-Frias et al., 2000).

Tail growth is a function of a specialized region of ectoderm, the ventral ectodermal ridge (VER), which acts analogously to the apical ectodermal ridge (AER) of the limb bud. Both the AER and VER signal adjacent mesodermal tissues to maintain an undifferentiated state, facilitating growth and elongation (Goldman et al., 2000; Saunders, 1948). The VER forms before morphological tail development (St. 18 in chick (Mills and Bellairs, 1989) and E10 or 35+ somites in the mouse (Gruneberg, 1956)) from the cloacal membrane posterior to the tailbud where ecotoderm and endoderm are justaposed (Gruneberg, 1956). During the ensuing gastrulation events the tailgut develops anterior to the cloacal membrane and elongates in close association with the tail and in close proximity to its ectoderm. Apoptotic

degeneration of the tailgut endoderm and VER heralds completion of tail growth (Fallon and Simandl, 1978; Miller and Briglin, 1996; Mills and Bellairs, 1989).

Despite common tail formation in early vertebrate development, tail growth ceases at different developmental time points in a species specific manner. Tail length is a characteristic phenotype amongst species yet its molecular controls are unknown. Molecular candidates include the *Hox* genes, homeobox containing transcription factors that function in pattern formation of many aspects of development (Krumlauf, 1994). In vertebrates the Hox genes are expressed in a characteristic spatial and temporal pattern mirroring their physiocal location in the chromosome. The most 5' *Hox* genes are expressed in the posterior body region including the posterior **mesodermal** regions of the gut (Roberts et al., 1995; Yokouchi et al., 1995b). These play an important role in patterning the gut along the anterior-posterior axis (AP) (Roberts et al., 1995; Roberts et al., 1998; Warot et al., 1997). *Hoxa13* and *Hoxd13* are expressed specifically in the cloacal mesoderm and also uniquely in the hindgut and cloacal endoderm (Roberts et al., 1995; Yokouchi et al., 1995b). Their endodermal function is unknown.

Mutations in *Hox**a**13,* both spontaneous and transgenic, exist in mice (Goodman and Scambler, 2001). The mutant phenotypes show both limb and GGU anomalies. Spontaneous murine *Hox**a**13* mutant, *hypodactyly* (*hd*), has a 50 base pair deletion within the first exon of *Hox**a**13* resulting in a mutant fusion protein (Mortlock et al., 1996). Although these mice suffer a high perinatal mortality, some homozygotes survive but are infertile due to hypoplasia of distal reproductive structures (Warot et al., 1997). As the *Hox**a**13* null mice are early perinatal lethal (Fromental-Ramain et al., 1996) the *hd* protein may act as a gain of function mutant.

Murine *Hox**d**13*-/- male show subtle GU anomalies (Dolle et al., 1993; Kondo et al., 1996; Podlasek et al., 1997) and homozygotes have abnormalities of the lowest sacral vertebra (Dolle et al., 1993). *Hox**d**13*-/+ embryos crossed with *Hox**a**13* null heterozygotes, have GGU anomalies more severe than in the *Hox**d**13*-/- alone suggesting that cooperation and redundancy between *Hox**a**13* and *Hox**d**13* exists in their function in GGU development (Warot et al., 1997).

Missense and nonsense mutations of one allele of *Hox**a**13* cause hand-foot-genital (HFG) syndrome (Goodman and Scambler, 2001), a rare dominantly inherited human disease{MIM 14000}. Affected individuals have mild, fully penetrant, symmetrical, bilateral hand and foot anomalies. Affected individuals also exhibit incompletely penetrant and variably severe genitourinary tract (GU) abnormalities including hypospadias in males and Müllerian duct fusion abnormalities in females. Both sexes show abnormalities in ureter/bladder placement. The variety of mutations described includes deletions, truncations of the protein, or amino acid substitutions within the conserved homeodomain. The resulting proteins are thought to act either as a gain-of function mutation or possibly a competitor of the wild-type protein.

Mutations in human *Hox**d**13* cause a severe distal limb phenotype termed synpolydactyly (SPD) {MIM 186000}. This rare, dominantly inherited syndrome is caused by mutations in a polyalanine repeat within the coding region of *Hox**d**13*, including expansions and intragenic deletions (Goodman and Scambler, 2001). Affected males often demonstrate GU abnormalities (Goodman and Scambler, 2001).

The manner in which these *Hoxa13* and *Hoxd13* mutations and nulls lead to these specific GGU malformations is unknown and may be due to either or both a mesodermal or

endodermal effect of the mutation. Murine models to date have failed to address their possible tissue specific functions.

To study the role of *Hoxa13* in GGU development we used the chick embryo model system. We studied the specific endodermal role of *Hoxa13* using the avian specific retroviral expression system and in ovo electroporation to overexpress wild-type and mutant forms role of *Hoxa13* in the chick hindgut endoderm in ovo. We constructed a chick *Hoxa13* homolog of one of the specific mutations that causes HFG (*HFGa13*). We chose the originally described *Hoxa13* mutation in which a small deletion of the Cterminal results in truncation of the protein (Morlock and Innis 1997). When expressed in the chick posterior endoderm a dramatic GGU and tail malformation results. We show that this effect is specific to **endodermal** *HFGa13* expression. We show that HFGa13 likely acts by interfering with the normal function of endogenous Hoxa13 and Hoxd13.

MATERIALS AND METHODS

Embryos: Timed fertilized white leghorn eggs (SPAFAS, CT) were incubated at 38^0C in a humidified incubator (Kuhl,NJ) until used experimentally. Embryos were staged according to Hamburger and Hamilton (St.) (Hamburger and Hamilton, 1951) or by embryonic day (E).

Constructs: Isolation of chicken *Hoxa13* gene has been previously described (Nelson et al., 1996). Although this clone was thought to be a full-length cDNA, a recent manuscript described evolutionarily conserved 3' sequence which was not present in our original clone (Mortlock et al., 2000). We isolated this N-terminal sequence by RT-PCR on E6 hindgut

total RNA with a primer designed to amplify the conserved 3' sequence (ATGTTCCTCTACGACAACAGC). After sequence verification and subcloning we verified the full-length chick *Hoxa13* cDNA.

By PCR we mutated chick *Hoxa13* to produce a truncation similar to a specific human mutation (*HFGa13*). Mutated reverse oligonucleotide (TCAGATTGTGACCTGTCGC) produced a premature stop codon as described by Mortlock (Mortlock and Innis, 1997).

Wild-type *Hoxa13* and *HFGa13* cDNAs RCAS(A) or RCAS(B) viruses and a *Hoxd13* RCAS(A) virus were produced as described (Morgan and Fekete, 1996). We found no difference in any of the experimental results described below using either the short or long form *Hoxa13* or *HFGa13* and, therefore, we do not distinguish between them herein. Similarly, 3' long and short forms of RCAS(A)*Hoxd13* acted equivalently in a chick limb bud overexpression study (Goff and Tabin, 1997). We found no difference in the infectivity of either A or B envelope coats of RCAS, both acted equivalently.

Constructs for electroporation were prepared with wild-type *Hoxa13* and *HFGa13* cDNAs cloned into pCDNA3 (Invitrogen). An N-Flag epitope oligonucleotide was inserted in frame with the GAL4 DNA Binding Domain (Sadowski and Ptashne 1989). All sequences were confirmed prior to use in experiments.

Transfection studies and Western blots: Plasmids used for transfections were purified using the maxiprep reagent system (Qiagen). COS-7 at 60-80% confluence were washed twice with serum-free medium and then co-transfected with 100 ng of reporter plasmid (pG5*luc* containing 5 GAL4 binding site (Promega)), 10 ng of Renilla luciferase promoter

vector (Promega), and 100 ng of different *Hoxa13* plasmids with 3µl of LipofectAMINE (Life Technologies) in 200 µl of serum-free medium. After 30 minutes of incubation, 500 µl of medium supplemented with 10% serum was added. Cells were harvested after 36 h of culture. Luciferase assays were checked with the Dual-Luciferase™ Reporter Assay (Promega). Promoter activities were expressed as relative luciferase activity: units/Renilla units, and each values represents the mean of six separate wells.

Relative expression of the GAL4 fusion proteins was assessed by Western-blot analysis of COS-7 extracts. Transfections with wild-type *Hoxa13* and *HFGa13* constructs fused to GAL4 DNA Binding Domain (DBD) were done as described previously (Sadowski and Ptashne 1989). GAL4 DBD antibody (Santa Cruz Biotech, Inc.) was used as described by the manufacturer.

Cells were fixed 24 h after transfection for 30 min in 4% paraformaldehyde in 0.1 M phosphate-buffered saline (PBS), permeabilized with PBS containing 0.02% Triton X-100, and incubated in 10% normal goat serum in PBS for 30 min at RT. Cells were then incubated with an anti-FLAG M5 monoclonal antibody (Kodak; 1:500) for 2 h at RT, followed by incubation with secondary antibody. Images were collected and processed on a Microphot Nikon microscope.

Viral infection: This technique has been previously described (Morgan and Fekete, 1996). Embryos at St.8-10 were used for experiments of the posterior endoderm, St.18 for experiments in the limb. Approximately 1-5µl of freshly defrosted virus dyed with fast green was injected per embryo. For hindgut experiments, the virus was injected into the region lateral and posterior to the tailbud following a published fate map (Matsushita, 1999). Double

injections were performed by mixing equal volumes of each viral aliquote before injection, as previously described (Bendall et al., 1999). In all cases, the *HFGa13* virus was cloned in RCAS(B) and the wild-type viruses were in RCAS(A). For limb injections, the right hindlimb bud was viewed at St.18. Approximately 1-5µl of virus was injected filling the entire limb bud. Eggs were then placed at 38^0C until harvest. Viral constructs injected included short and long forms (see above) of wild-type *Hoxa13*, *HFGa13* and, as controls, wild-type *Hoxd13* and *GFP*. More than 10 dozen embryos were injected with each construct.

Electroporation: This technique was adapted to a technique previously published (Grapin-Botton et al., 2001). E2.5 (St. 11-14) embryos were used for electroporation, at CIP invagination and tailbud formation. Plasmids were diluted to a final concentration of 2 µg/ml in PBS adding 1 µM $MgCl_2$. To facilitate viewing of the viral aliquot and to slow diffusion, 50 µg/ml Nile Blue Sulfate, 3 mg/ml carboxymethylcellulose was added to the construct liquid. 5 to 10 µl of this solution was deposited using a microcapillary pulled micropipette positioned under embryo at the posterior most endoderm layer (just caudal to the tailbud). Quickly after injection, a cathode was positioned on the dorsal surface of the embryo at the level of the injected construct. The anode was placed parallel to the cathode under the embryo (about 3 mm deep) at the level of the injected construct. Neither electrode touched the embryo. Three square pulses of 17 Volts and 50 msec each were applied to the embryo (BTX T-280 square wave electroporator generously lent to us by the Melton Lab under supervision of Anne Grapin-Botton) to allow vector integration into the endodermal layer. Eggs were incubated at 38^0C until embryonic death or harvest. Controls included solution with all components except the vector, solution with empty vector, construct containing the

wild-type *Hoxa13,* or with vector containing *GFP* only. Approximately 3 dozen eggs were electroporated in experimental and control groups.

Whole embryo explants: The technique was adapted from that of Chapman et al. (Chapman et al., 2001). Dissected St. 9-13 embryos were placed ventral side up in a freshly made thin layer of albumin/agarose (Chapman et al., 2001). Using a dissecting microscope (Olympus SZH10) the posterior endoderm covering the tailbud and posterior was removed using one of these techniques: dissection alone using pulled glass needles and fine forceps, enzymatic digestion using 0.03% collagenase in PBS dropped on the embryo over the tailbud and allowed to sit for 15 minutes at 37^0C and washed with 5 drop/aspirate cycles using PBS+10% chick serum followed by 5 drop/aspirate cycles using PBS + pen/strep, or a combination of both techniques. Controls had no manipulation. Transplanted embryos had caudal endoderm removed as above. Donor endoderm was removed from donor stage 17 embryos (for facility and to ensure good *Hoxa13* expression by the posterior endoderm) by sharp dissection, kept oriented, and divided into thirds along the AP axis. The anterior endoderm and posterior endoderm were isolated and transplanted to host embryos (separately) by transfer pipette and forceps. Embryos were harvested immediately after manipulation, and at 24 and 48 hours. For each condition at least 12 embryos were used over five separate experiments.

Analysis: Embryos were harvested and fixed in freshly made 4% paraformaldehyde in PBS for 4-20 hours. Fixed embryos were washed in PBS and then either taken through a graded series of methanol-PBS to 100% methanol and kept at -20^0C, until used for whole mount in situ hybridization studies, or were frozen in cryomount (Fisher Scientific) for cryosectioning.

Whole mount in situ hybridization studies followed our published technique (Roberts et al., 1998). 10 μm cryosections on Superfrost Plus slides (Fisher Scientific) were air dried for 4-18 hours and kept at -20^{0}C until used. Some fixed, in situ hybridized embryos were embedded in paraffin and sectioned at 5 μm for histologic analysis. Haematoxylin and eosin (H&E) staining was performed using standard techniques. Section in situ hybridizations were performed using published techniques (Smith et al., 2000). Immunohistochemical stains were performed using standard techniques and the Vectastain ABC detection system (Vector Laboratories, Inc) following the manufacturer's directions. Hoxa13 antibody was a generous gift from A. Kuroiwa and used as previously described (Yokouchi et al 1995a). 3C2 antibody specific to RCAS GAG protein has been published before (Smith et al, 2000). Ribroprobes were transcribed using Roche ribroprobe synthesis kits per the manufacturer's directions. All riboprobes used herein have been previously published (Nielsen et al., 2001; Roberts et al., 1995; Roberts et al., 1998; Smith et al., 2000; Vogel et al, 1996).

Genbank accession number AY030050. Gallus gallus *Hoxa13*.

RESULTS

Spatio-temporal expression of *Hoxa13* during posterior GGU/tail development

Hoxa13 is first expressed early in the most posterior part of the embryo, adjacent to Hensen's node in the area that will give rise to the CIP (St. 10) (Fig. 1A). *Hoxa13* is expressed at St. 14 in the CIP (Fig. 1B). Later, *Hoxa13* expression is restricted to the dorsal mesoderm of the tailbud, cloacal mesoderm, hindlimb bud mesoderm, and caudal endoderm (Fig. 1C,D). *Hoxa13* and its product are strongly expressed in the endoderm of the hindgut

and cloaca through early development of the gut (Fig. 1E,F) (Roberts et al., 1995; Yokouchi et al., 1995b).

Human HFG and chick HFGa13 overexpressed embryos have similar phenotypes

Overexpression of *Hoxa13* in the posterior embryo failed to produce a tail or gut phenotype. We did see an epithelial transformation (from midgut to hindgut) when midgut mesodermal tissues expressed *Hoxa13* (see Fig. 7H for comments) as was described with ectopic *Hoxd13* expression in the midgut (Roberts et al., 1998).

To determine if expression of chick mutated *Hoxa13* (*HFGa13*) results in a phenotype similar to that observed in the human HFG syndrome, we chose to construct a similar nonsense mutation as described by Mortlock and Innis, 1997. The Cterminal mutation leads to a production of a mutated Hoxa13 protein, with the last 20 last amino acids deleted. We expected that HFGa13 protein would be able to interfere with the endogenous Hoxa13.

In order to test our hypothesis, we first misexpressed *HFGa13* in the hindlimb, and we were able to produce a severe morphological change reminiscent of limb defect described in HFG syndrome (Fig. 2A). The *HFGa13* expressing hindlimb shows a specific malformation characterized by a substantial reduction in limb size in both the anterioposterior and dorsoventral axes compared to the uninfected contralateral control limb. *HFGa13* E6 infected hindlimbs revealed a specific skeletal hypoplasia of the fibula (without changes in the tibia) and a reduction of the entire autopod area (Fig. 2A,B). This phenotype suggested a late disruption of the apical ectodermal ridge (AER). Consistent with this, *Fgf8* mRNA expression was not detectable in the distal hindlimb AER of the *HFGa13* hindlimbs (Fig. 2C). The distal fibular cartilage fails to properly develop and remains undifferentiated

mesenchymal cells. Expression of *Bapx1* was decreased only in the malformed fibula (Fig. 2D). No AER disruption or fibula maldevelopment were observed with the wild-type *Hoxa13* overexpression (data not shown). These results suggest that *HFGa13* interferes with the maintenance of the AER in the hindlimb and with formation of the fibula. We conclude that our construct functions to give a chick phenocopy of the human HFG syndrome.

Endodermally expressed *HFGa13* causes abnormal hindgut and tail development

HFGa13 and control constructs were expressed in the chick *in ovo* by injection of virus, targeting the prospective hindgut in St. 8-10 embryos. We used this targeting technique previously to infect the midgut mesoderm (Roberts et al., 1998), but in the experiments described herein we often found strong endodermal infection in the hindgut as well (Fig. 3B).

Specific gross morphologic defects were obtained only with *HFGa13* infections and only when the infection included the posterior endoderm (Fig. 3A,B). *Hoxa13, Shh, Bmp4,* and *GFP* constructs failed to produce this phenotype ever, even when expression was noted in the endoderm (data not shown). *HFGa13* infected in the mesodermal only were phenotypically normal (Fig. 3 C,D). Our survival rate was 50-80% depending on time of incubation (survival to E3 better than to E18). Approximately 20% of *HFGa13* injected embryos demonstrated the mutant phenotype. All *HFGa13* embryos were analyzed for viral infection. All mutant embryos harbored posterior endodermal and mesodermal virus expression. Those without the phenotype showed no viral infection or only posterior mesodermal virus expression (no infection in the endoderm).

To determine if endodermal expression of *HFGa13* is sufficient to obtain these posterior defects we used an in ovo electroporation technique (Grapin-Botton et al., 2001).

Three groups of E2.5 (St. 11-16) embryos were electroporated: control group with empty vector or a *GFP* containing vectors, those with wild-type *Hoxa13* construct; and finally a group with *HFGa13*. In E5 survivors, posterior short tail/hindgut atresia was present *only* in the *HFGa13* electroporated embryos, electroporation of control constructs produced no defects (data not shown). The mutant phenotype was restricted to those embryos with hindgut epithelial expression of *HFGa13* (electroporations restricted to the midgut endoderm failed to produce the posterior phenotype (data not shown)).Survival was about 80% for all groups. The posterior endodermal *HFGa13* expressing embryos show similar, albeit more severe, defects as those obtained using the injection/infection technique (Fig. 3E). Confirmation of tissue integration and endodermal tissue survival were performed by tag immunostaining on all embryos (Fig. 3F). Sections of experimental embryos confirmed an intact endoderm an a histologically normal neural tube and notochord (Fig. 4). Approximately 10 embryos showed the phenotype (all the survivors and all the embryos with documented expression in the hindgut endoderm).

Histological analyzes of mutant *HFGa13*-infected embryos were done by H&E staining. The phenotype includes malformations of the hindgut and tail (Fig. 4A,C,E and G) including maldevelopment of the tail somites and a short tail (compare Fig. 4A,C respectively with B,D). Hindgut defects include atresia of the anterior to the cloaca (compare Fig. 4E with F), malformed and malpositioned posterior cloaca (compare Fig. 4C,K respectively with D,L). Additional defects are noted in other cloaca-associated viscera including cystic mesonephric maldevelopment with normal non-atretic ureters and atresia of the distal Müllerian ducts (compare Fig. 4G with H). No associated neural tube defects or malformations are present (as shown in Fig. 4). We occasionally obtained a severe

phenotype, termed ourentery (Rabaud 1900), in which the tail appears to have grown ventrally and internally to the remaining cloacal orifice, often accompanied with ventral internal malpositioning of tail structures into the hindgut and internalization of the allantois (compare Fig. 4A,C with B,D and also Fig. 3B with 3D). All these results show that *HFGa13* expression, specifically in the posterior endodermal, induces maldevelopment of many of the caudal structures.

HFGa13 affects expression of *Hoxd13*, *Fgf8* and *Bapx1*

Molecular analysis of *HFGa13* mutant embryos were made with specific dorsoventral (DV), anteroposterior (AP), and cytodifferentiation markers. Strong down-regulation was observed with VER marker *Fgf8* (ectoderm and mesoderm) and with AP marker *Hoxd13* (mesoderm and endoderm) (respectively Fig. 5A and D). *Bapx1* shows a diminished expression in the short tail (Fig. 5B). No change was noted in the expression of ventral mesodermal markers: *Wnt5a* (Fig. 5C) and *Bmp4* (data not shown) and normal expression of *Shh* (Fig. 5E).

Caudal gut endodermal signals are needed for normal posterior gut and tail development

To test our hypothesis that posterior gut and tail development requires specific *endodermal* signals we used whole embryo explant cultures in which we removed the endoderm at early (pre-CIP) stages (St. 9-11). Survival (90% of un-manipulated controls, 75% of manipulated embryos) after 2 days, to St. 20 allowed analysis of tail development. None of the control embryos had caudal defects (Fig. 6A). All embryos in which the caudal endoderm had been removed showed severe caudal defects of the tail and gut. Those

embryos that survived to form hindlimb buds generally formed abnormal CIP and blunted tails similar to those produced in the *HFGa13* injected or electroporated embryos (Fig. 6B). Ourentery was present in 50% of manipulated survivors (Fig. 6C). No neural tube defect was present in these embryos.

When examined histologically, we confirmed that the midline ventral endoderm overlying the tailbud was removed (data not shown). This endoderm is absent for the first 24 hours after dissection then it appears that the adjacent endoderm occasionally re-grows over this defect (Fig. 6C). No defects are seen in the more anterior endoderm (Fig. 6D). To confirm that removal of the caudal endoderm was complete we analyzed the normal and abnormal embryos for the presence of early endodermal markers. In the caudal ventral tissues of normal embryos we found expression of *Shh, Cdxa* (Fig. 6E), and *Hoxa13* (Fig. 6A), and *Hoxd13* (data not shown). We also could not detect expression of these markers in the caudal ventral tissues of abnormal embryos at time points less than 24 hours (Fig. 6B,F). Rescue experiments included transplanting donor endoderm (either anterior or posterior) harvested from St. 17 embryos to the embryos in which the CIP endoderm had been removed. Only transplanted posterior endoderm rescued the tail and gut defect (Fig. 6G). Anterior endodermal transplants failed to rescue blunted tail phenotype (Fig. 6H). Our results show that the posterior endoderm produces signals necessary for normal tail and hindgut development.

HFGa13 interferes with the cellular functions of Hoxa13 and Hoxd13 proteins

To investigate the molecular pathway by which HFG *Hoxa13* mutation functions, transactivation activities of wild-type Hoxa13 and HFGa13 were first analyzed in

heterologous COS-7 cell line by luciferase assay using the synthetic GAL4 reporter system. Constructions for transfection studies were prepared using the pSG424 vector that contains the GAL4 DNA Binding Domain. Wild-type *Hoxa13*, *HFGa13* and *Hoxd13* cDNAs were subcloned into pSG424 vector in frame with the GAL4 DBD. We show that wild-type Hoxa13 protein fused to the GAL4 DNA-binding domain is able to activate transcription of this synthetic reporter (Fig. 7A). The HFGa13 construct is not able to activate the synthetic GAL4 promoter but we did notice a decrease in the basal activity using this construct. To verify expression and protein stability, we performed Western-blot analysis on whole COS-7 cell extracts of transfected cells using a specific GAL4 DBD antibody. We show that all these proteins were expressed at comparable levels as assayed by Western blotting, indicating that the inability to activate transcription is not linked to a lack of expression or instability of the HFGa13 proteins (data not shown). To determine whether a difference in intracellular localization of HFGa13 proteins could affect transcriptional activity, localization of N-flag-tagged proteins within transfected COS-7 cells was examined by immunostaining (Fig. 7C, D). Strong signals for wild type Hoxa13 and HFGa13 proteins were both observed in the nuclei of transfected COS-7 cells. However, a weak additional signal was detected in the cytoplasm with HFGa13.

Using the same synthetic GAL4 reporter system, we investigated the possible interactions between Hoxa13 and HFGa13. We used the same conditions with a plasmid containing *Hoxa13* and a GAL4 DBD, but added one plasmid containing *HFGa13* cDNA without GAL4 DBD (unable to bind the 5 GAL4 DBB repeats). Using this competition assay with same molar ratio we show that HFGa13 protein is able to decrease *Hoxa13* transcriptional activity (Fig. 7B). Increased amounts of HFGa13 increases the strength of the

repression. Interestingly, HFGa13 protein is also able to act in a dominant negative fashion with Hoxd13 by repressing Hoxd13 transcriptional activity (Fig. 7B).

In order to determine if *HFGa13* acts as a dominant negative *in vivo* we used a competitive assay taking advantage of an epithelial phenotype alteration induced by overexpression of the wild-type *Hoxa13* in the midgut. At E18, epithelium differentiation is nearly complete. Midgut epithelium is characterized by long and thin villi (Fig. 7E) whereas hindgut epithelium shows wide and flat villi (Fig. 7F). We have previously shown that ectopic *Hoxd13* expression in the midgut mesoderm causes the midgut epithelium to develop with a hindgut/cloacal phenotype (Roberts et al, 1998). Herein we show that the same epithelial tranformation occurs with *Hoxa13* misexpression in the midgut mesoderm (Figure 7H and J). However, infection of the midgut with *HFGa13* did not transform the epithelium (Fig. 7G). If our *HFGa13* acts as a dominant negative, then it should be able to repress the midgut epithelial transformation induced by ectopic *Hoxa13* or Hoxd13 expressions in the midgut mesoderm. In order to test our hypothesis, we co-infected mesodermal midgut with RCAS(B)-*HFGa13* and RCAS(A)-*Hoxa13* or *Hoxd13* retrovirus in equal titer. We used different RCAS envelope proteins to facilitate cellular co-infection as previously described (Morgan and Fekete 1996; Bendall et al., 1999). All these midgut were processed with 3c2 immunostaining to detect mesodermal virus expression (data not shown, Fig. 7L). In order to valid our co-infection experiments, we checked for viral co-expressions of both virus, and always were able to correlate viral mesodermal midgut infection (shown by 3c2 immunstaining) with ectopic co-expression of both *HFGa13* and *Hoxd13* (Fig. 7L). Co-infections of *HFGa13* with *Hoxa13* (Fig. 7I) or *Hoxd13* (Fig. 7K) are sufficient to inhibit the action of *Hoxa13* or *Hoxd13* (compare respectively Fig. 7H with I, and Fig. 7J with K).

These experiments indicate that this HFG nonsense mutation likely functions as a dominant negative. HFGa13 may compete with the endogenous function of wild-type Hoxa13 and/or Hoxd13 proteins in vivo as a dominant-negative, like that observed with the human patient heterozygous for this mutation, probably by interfering with protein partners and/or transcriptional machinery.

DISCUSSION

It has been known for some time that there is a close association between the development of the gut and the tail or related structures (coccyx and sacral vertebrae). Human congenital malformations in one often affect the other systems. This association is seen in spontaneous and transgenic malformations in many vertebrate species (Maatman et al., 1997; Warot et al., 1997). The GGU and tail tissues derive from the tailbud mesenchyme proably via secondary body formation (Griffith et al., 1992). The factors involved in this process, if mutated, may affect multiple caudal structures. There is evidence to support this both experimentally and spontaneously produced in many vertebrate systems. When portions of the tailbud are removed early in chick development, tail truncations and cloacal anomalies are common (Schoenwolf, 1978). In some specific spontaneous murine mutants with tail truncation anomalies, GGU malformations are common, for example, Danforth's Short Tail mutant (*sd*) develops anal stenosis, rectal duplications, anal atresias in association with the characteristic short tail (Dunn et al., 1940). In humans, the relationship between sacral and coccygeal vertebral defects and hindgut defects has also been documented (van der Putte, 1986) in sporadic/isolated malformations (eg. cloacal and bladder exstrophy (Loder and

Dayioglu, 1990; Martinez-Frias et al., 2000)) and syndromic malformations (e.g. VATERCL syndrome that includes anal atresia and hemivertebrae (Beals and Rolfe, 1989). Another example is the limb/pelvis-hypoplasia/aplasia syndrome that includes absent fibulae, Müllerian aplasia, and sacral hypoplasia (Raas-Rothschild et al., 1988)). The elucidation of the mechanism of this association has been difficult, likely due to the complexity of the malformations as the malformations often involve anomalies of all three germ layers, deciphering the primary from the secondary effects in a transgenic model is troublesome.

Tail development is universal amongst vertebrates, although the persistence of a tail is not. Tail length is a function of the developmental time point that tailgut and VER apoptosis occurs. We suggest a functional relationship between the caudal endoderm and the VER. Gruneberg suggested that the origin of the VER is from the cloacal membrane (Gruneberg, 1956). Other experimental evidence supports the association between caudal endoderm and the VER. VER ablation causes a displacement of the tailgut dorsally due to increasing the number of cells between the VER and tailgut (Goldman et al., 2000). In murine chimeras derived from wild-type and *sd* mutant ES cells it was shown that the *sd* cells never populated the ventral hindgut or tailgut suggesting a ventral signal from the gut endoderm is absent in the *sd* mutant mouse (Maatman et al., 1997). It may be that the impairment of heterozygous and homozygous *sd* mutant cells to colonize the ventral hindgut endoderm is the earliest manifestation of the *sd* phenotype (Maatman et al., 1997).

The molecular controls of normal or abnormal tail/GGU are poorly understood but VER function and signals have recently been described (Goldman et al., 2000). Signals from specialized ectoderm in the limb (AER) and the tail (VER) direct elongation of their respective subjacent structures. The AER and VER do not appear to be functionally

equivalent. In mice, both the AER and VER express a fibroblast growth factor and a bone morphogenic protein (Dudley and Tabin, 2000; Maatman et al., 1997). Although exogenous application of FGF or BMP to the AER rescues the limb phenotype in AER ablated embryos (Zuniga et al., 1999), these proteins when placed on VER ablated tails in vitro failed to rescue the blunted tail phenotype (Goldman et al., 2000). Transplanting the AER to VER ablated tails also fails in rescuing growth (Goldman et al., 2000). There are clearly other factors, either from the VER or other tail tissues that are important in directing tail development. We conclude that signaling between the endoderm and ectoderm at this very early stage of development is critical and independent of notochord or neural tube related inductions. We suggest that one of these factors is *Hoxa13* derived from the caudal endoderm.

Clearly there are multiple factors involved in tail development. Many different model systems–genetic, mechanical, and toxic can result in the phenotype of blunted tail and cloacal anomalies. Classical anatomic literature has examples of toxic or pharmacological induction of blunted tail and ourenteric malformations in chick including exposure to insulin (Moseley, 1947), organophosphides (Wyttenbach and Thompson, 1985), and retinoic acid (Griffith and Wiley, 1989). Mechanical disruptions by transection or extirpation of the notochord, tailbud, and hindgut endoderm, shaking, or placement of a conductive glass tube all result in blunted tail and ourentery (Moseley 1947) and references therein, (Hotary and Robinson, 1992). The transgenic data in mice shows that pertubations in many different pathways result in blunted tails including FGF (Furthauer et al., 1997), BMP (Brunet et al., 1998), Wnt (Yamaguchi et al., 1999), and retinoic acid (Abu-Abed et al., 2001). What is common to these diverse "methods" of producing the combination of caudal tail/vertebrae and gut defects? We suggest

one possibility may be interruption of caudal endoderm signaling needed for normal tail development.

A spontaneous genetically dominant chicken mutation resembles the phenotype of our *HFGa13* embryos. Dominant *Rumpless* chicks develop a truncated tail, abnormal cloaca, and often show ourentery (Zwilling, 1942). It would be very interesting to determine if *Hoxa13* is mutated or if abnormalities in this pathway are present in this strain. We are currently studying dominant rumpless chick embryos for *Hoxa13* mutations.

In the human syndrome HFG, no sacral or coccygeal anomalies have been reported. In the murine counterpart, *hd* shows anal stenosis but not caudal vertebrae or tail defects (Post and Innis, 1999). Interestingly, caudal vertebrate malformations due to mutations in the paralog *Hoxd13*, though, have been reported ***both*** in human SPD syndrome (Akarsu et al., 1996) and in homozygous *Hoxd13* knockout mice (Dolle et al., 1993). We show that our HFGa13 construct interferes with the normal expression and function of *Hoxd13* (Figs. 5 and 7). Our *HFGa13* phenotype may be in part an indirect phenomenon due to downregulation of *Hoxd13*.

It is curious that the human, chick, and murine phenotypes differ given the same genetic alteration. It may be that there are subtle vertebral defects in human individuals with HFG not described to date. Similarly, subtle murine lumbosacral or tail abnormalities may have escaped observation in the *hd* or *Hoxa13*-/- mice. Our findings in chick may relate to the particular *Hoxa13* mutation we constructed or to the relative levels of wild-type and mutant proteins in the "transgenic" embryos. Or, it may be due to a different function of *Hoxa13* in avian species in the posterior vertebrae compared with that of mouse and human.

A theory derived from our results suggests that the presence of a tail structure in a vertebrate species may be related to persistence of the tailgut during development. In humans and avians the tailgut undergoes apoptotic regression relatively early in development (Fallon and Simandl, 1978; Miller and Briglin, 1996), whereas in rodents the tailgut persists over a much longer relative developmental time period (Goldman et al., 2000). Although this study does not address the upstream controls of *Hoxa13* expression in this caudal region, it follows that significant differences in this control would exists amongst species with different tail lengths.

Acknowledgements

We thank C. Nielsen, S. Winfield, and T. Manganaro for technical assistance. We thank C. Tabin and P. Donahoe for generous guidance, use of reagents, and expertise. We thank G. Schoenwolf, L. Pierro, and F. Goldman for helpful discussions and insights into our results. We are especially appreciative of direct guidance and sharing of equipment from D. Melton and A. Grapin-Botton. We are indebted to A. Kuroiwa and his laboratory for generous sharing of the precious Hoxa13 antibody. Thanks to S. Faure and A. de Santa Barbara for support. This work was supported by NIH grant HD34448-03 to D.J.R. to P.d.S.B. an ARC postdoctoral fellowship and an American Foundation of Urology Fellowship Grant.

REFERENCES

Abu-Abed, S., Dolle, P., Metzger, D., Beckett, B., Chambon, P. and Petkovich, M. (2001). The retinoic acid-metabolizing enzyme, CYP26A1, is essential for normal hindbrain patterning, vertebral identity, and development of posterior structures. *Genes Dev* **15**, 226-40.

Akarsu, A. N., Stoilov, I., Yilmaz, E., Sayli, B. S. and Sarfarazi, M. (1996). Genomic structure of HOXD13 gene: a nine polyalanine duplication causes synpolydactyly in two unrelated families. *Hum Mol Genet* **5**, 945-52.

Beals, R. K. and Rolfe, B. (1989). VATER association. A unifying concept of multiple anomalies. *J Bone Joint Surg Am* **71**, 948-50.

Bendall, A. J., Ding, J., Hu, G., Shen, M. M. and Abate-Shen, C. (1999). Msx1 antagonizes the myogenic activity of Pax3 in migrating limb muscle precursors. *Development* **126**, 4965-76.

Brunet, L. J., McMahon, J. A., McMahon, A. P. and Harland, R. M. (1998). Noggin, cartilage morphogenesis, and joint formation in the mammalian skeleton. *Science* **280**, 1455-7.

Catala, M., Teillet, M. A. and Le Douarin, N. M. (1995). Organization and development of the tail bud analyzed with the quail- chick chimaera system. *Mech Dev* **51**, 51-65.

Chapman, S. C., Collignon, J., Schoenwolf, G. C. and Lumsden, A. (2001). Improved method for chick whole-embryo culture using a filter paper carrier. *Dev Dyn* **220**, 284-9.

Dolle, P., Dierich, A., LeMeur, M., Schimmang, T., Schuhbaur, B., Chambon, P. and Duboule, D. (1993). Disruption of the Hoxd-13 gene induces localized heterochrony leading to mice with neotenic limbs. *Cell* **75**, 431-41.

Dudley, A. T. and Tabin, C. J. (2000). Constructive antagonism in limb development. *Curr Opin Genet Dev* **10**, 387-92.

Dunn, L., Gluecksohn-Schoenheimer, S. and Bryson, V. (1940). A new mutation in the mouse affection spinal column and urogenital system. *J Hered* **31**, 343-348.

Fallon, J. F. and Simandl, B. K. (1978). Evidence of a role for cell death in the disappearance of the embryonic human tail. *Am J Anat* **152**, 111-29.

Fromental-Ramain, C., Warot, X., Messadecq, N., LeMeur, M., Dolle, P. and Chambon, P. (1996). Hoxa-13 and Hoxd-13 play a crucial role in the patterning of the limb autopod. *Development* **122**, 2997-3011.

Furthauer, M., Thisse, C. and Thisse, B. (1997). A role for FGF-8 in the dorsoventral patterning of the zebrafish gastrula. *Development* **124**, 4253-64.

Gajovic, S., Kostovic-Knezevic, L. and Svajger, A. (1993). Morphological evidence for secondary formation of the tail gut in the rat embryo. *Anat Embryol (Berl)* **187**, 291-7.

Goff, D. J. and Tabin, C. J. (1997). Analysis of Hoxd-13 and Hoxd-11 misexpression in chick limb buds reveals that Hox genes affect both bone condensation and growth. *Development* **124**, 627-36.

Goldman, D. C., Martin, G. R. and Tam, P. P. (2000). Fate and function of the ventral ectodermal ridge during mouse tail development. *Development* **127**, 2113-23.

Goodman, F. R. and Scambler, P. J. (2001). Human HOX gene mutations. *Clin Genet* **59**, 1-11.

Grapin-Botton, A., Majithia, A. R. and Melton, D. A. (2001). Key events of pancreas formation are triggered in gut endoderm by ectopic expression of pancreatic regulatory genes. *Genes Dev* **15**, 444-54.

Griffith, C. M. and Wiley, M. J. (1989). Direct effects of retinoic acid on the development of the tail bud in chick embryos. *Teratology* **39**, 261-75.

Griffith, C. M., Wiley, M. J. and Sanders, E. J. (1992). The vertebrate tail bud: three germ layers from one tissue. *Anat Embryol* **185**, 101-13.

Gruneberg, H. (1956). A ventral ectodermal ridge of the tail in mouse embryos. *Nature* **177**, 787-788.

Hamburger, V. and Hamilton, H. L. (1951). A series of normal stages in the development of the chick embryo. *J. Morph.* **88**, 49-92.

Holmdahl, D. E. (1925). Experimentelle untersuchungen uber die lage der grenze zwischen primarer and sekundarer korperentwicklung beium huhn. *Anat Anz Bd* **59**, 393-396.

Hotary, K. B. and Robinson, K. R. (1992). Evidence of a role for endogenous electrical fields in chick embryo development. *Development* **114**, 985-96.

Kluth, D., Hillen, M. and Lambrecht, W. (1995). The principles of normal and abnormal hindgut development. *J Pediatr Surg* **30**, 1143-7.

Knezevic, V., De Santo, R. and Mackem, S. (1998). Continuing organizer function during chick tail development. *Development* **125**, 1791-801.

Kondo, T., Dolle, P., Zakany, J. and Duboule, D. (1996). Function of Posterior *HoxD* genes in the morphogenesis of the anal sphincter. *Development* **122**, 2651-2659.

Krumlauf, R. (1994). Hox genes in vertebrate development. *Cell* **78**, 191-201.

Loder, R. T. and Dayioglu, M. M. (1990). Association of congenital vertebral malformations with bladder and cloacal exstrophy. *J Pediatr Orthop* **10**, 389-93.

Maatman, R., Zachgo, J. and Gossler, A. (1997). The Danforth's short tail mutation acts cell autonomously in notochord cells and ventral hindgut endoderm. *Development* **124**, 4019-28.

Martinez-Frias, M. L., Bermejo, E. and Rodriguez-Pinilla, E. (2000). Anal atresia, vertebral, genital, and urinary tract anomalies: a primary polytopic developmental field defect identified through an epidemiological analysis of associations. *Am J Med Genet* **95**, 169-73.

Matsushita, S. (1999). Fate mapping study of the endoderm in the posterior part of the 1.5-day- old chick embryo. *Dev Growth Differ* **41**, 313-9.

Miller, S. A. and Briglin, A. (1996). Apoptosis removes chick embryo tail gut and remnant of the primitive streak. *Dev Dyn* **206**, 212-8.

Mills, C. L. and Bellairs, R. (1989). Mitosis and cell death in the tail of the chick embryo. *Anat Embryol* **180**, 301-8.

Morgan, B. A. and Fekete, D. M. (1996). Manipulating gene expression with replication-competent retroviruses. In *Methods in avian embryology*, vol. 51 (ed. M. Bronner-Fraser), pp. 185-218. San Diego: Academic Press.

Mortlock, D. P. and Innis, J. W. (1997). Mutation of HOXA13 in hand-foot-genital syndrome. *Nat Genet* **15**, 179-80.

Mortlock, D. P., Post, L. C. and Innis, J. W. (1996). The molecular basis of hypodactyly (Hd): a deletion in Hoxa 13 leads to arrest of digital arch formation. *Nat Genet* **13**, 284-9.

Mortlock, D. P., Sateesh, P. and Innis, J. W. (2000). Evolution of N-terminal sequences of the vertebrate HOXA13 protein. *Mamm Genome* **11**, 151-8.

Moseley, H. R. (1947). Insulin-induced remplessness of chickens IV. Early embryology. *J Exp Zool* 1**05**, 279-316.

Nelson, C. E., Morgan, B. A., Burke, A. C., Laufer, E., DiMambro, E., Murtaugh, L. C., Gonzales, E., Tessarollo, L., Parada, L. F. and Tabin, C. (1996). Analysis of Hox gene expression in the chick limb bud. *Development* **122**, 1449-66.

Nielsen, C., Murtaugh, L. C., Chyung, J. C., Lassar, A. and Roberts, D. J. (2001). Gizzard formation and the role of Bapx1. *Dev Biol* **231**, 164-74.

Pasteels, J. (1943). Proliférations et croissance dans la gastrulation et la formation de la queue des vertébrés. *Arch Biol (Liège)* **54**, 1-51.

Podlasek, C. A., Duboule, D. and Bushman, W. (1997). Male accessory sex organ morphogenesis is altered by loss of function of Hoxd-13. *Dev Dyn* **208**, 454-65.

Post, L. C. and Innis, J. W. (1999). Infertility in adult hypodactyly mice is associated with hypoplasia of distal reproductive structures. *Biol Reprod* **61**, 1402-8.

Raas-Rothschild, A., Goodman, R. M., Meyer, S., Katznelson, M. B., Winter, S. T., Gross, E., Tamarkin, M., Ben-Ami, T., Nebel, L. and Mashiach, S. (1988). Pathological features and prenatal diagnosis in the newly recognised limb/pelvis-hypoplasia/aplasia syndrome. *J Med Genet* **25**, 687-97.

Rabaud, E. (1900). Etude embryologique de l'ourentérie et de la cordentérie. *Journal de L'Anat et de la Physiol* : 619-634 .

Roberts, D. J., Johnson, R. L., Burke, A. C., Nelson, C. E., Morgan, B. A. and Tabin, C. (1995). Sonic hedgehog is an endodermal signal inducing Bmp-4 and Hox genes during induction and regionalization of the chick hindgut. *Development* **121**, 3163-74.

Roberts, D. J., Smith, D. M., Goff, D. J. and Tabin, C. J. (1998). Epithelial-mesenchymal signaling during the regionalization of the chick gut. *Development* **125**, 2791-801.

Sadowski, I. and Ptashne, M. (1989). A vector for expressing GAL4(1-147) fusions in mammalian cells. *Nucleic Acids Res* **17**, 7539.

Saunders, J. W. (1948). The proximo-distal sequence of the origin of the parts of the chick wing and the role of the ectoderm. *J Exp Zool* **108**, 363-403.

Schoenwolf, G. C. (1977). Tail (end) bud contributions to the posterior region of the chick embryo. *J Exp Zool* **201**, 227-246.

Schoenwolf, G. C. (1978). Effects of complete tail bud extirpation on early development of the posterior region of the chick embryo. *Anat Rec* **192**, 289-95.

Schoenwolf, G. C. (1979). Histological and ultrastructural observations of tail bud formation in the chick embryo. *Anat Rec* **193**, 131-47.

S**mith, D. M., Nielsen, C., Tabin, C. J. and Roberts, D. J.** (2000). Roles of BMP signaling and Nkx2.5 in patterning at the chick midgut- foregut boundary. *Development* **127**, 3671-3681.

van der Putte, S. C. (1986). Normal and abnormal development of the anorectum. *J Pediatr Surg* **21**, 434-40.

Vogel, A., Rodriguea, C., Izpisua-Belmonte, J.C. (1996). Involvement of FGF-8 in initiation, outgrowth and patterning of the vertebrate limg. *Development* 122, 1737-1750.

Warot, X., Fromental-Ramain, C., Fraulob, V., Chambon, P. and Dolle, P. (1997). Gene dosage-dependent effects of the Hoxa-13 and Hoxd-13 mutations on morphogenesis of the terminal parts of the digestive and urogenital tracts. *Development* **124**, 4781-91.

Wyttenbach, C. R. and Thompson, S. C. (1985). The effects of the organophosphate insecticide malathion on very young chick embryos: malformations detected by histological examination. *Am J Anat* **174**, 187-202.

Yamaguchi, T. P., Bradley, A., McMahon, A. P. and Jones, S. (1999). A Wnt5a pathway underlies outgrowth of multiple structures in the vertebrate embryo. *Development* **126**, 1211-23.

Yokouchi, Y., Nakazato, S., Yamamoto, M., Goto, Y., Kameda, T., Iba, H. and Kuroiwa, A. (1995a). Misexpression of Hoxa-13 induces cartilage homeotic transformation and changes cell adhesiveness in chick limb buds. *Genes Dev* **9**, 2509-22.

Yokouchi, Y., Sakiyama, J. and Kuroiwa, A. (1995b). Coordinated expression of Abd-B subfamily genes of the HoxA cluster in the developing digestive tract of chick embryo. *Dev Biol* **169**, 76-89.

Zuniga, A., Haramis, A. P., McMahon, A. P. and Zeller, R. (1999). Signal relay by BMP antagonism controls the SHH/FGF4 feedback loop in vertebrate limb buds. *Nature* **401**, 598-602.

Zwilling, E. (1942). The development of dominant rumplessness in chick embryos. *Genetics* **27**, 641-656.

FIGURE LEGENDS

Fig. 1. Spatio-temporal expressions of *Hoxa13* (A-E) and Hoxa13 protein (F) during posterior GGU/tail development. (A) St. 10 (arrow at CIP). (B) St. 14 (arrow at CIP). (C) St. 17 (long arrows show tail tip, short arrow at hindgut and arrowhead at tailgut). Planes of cryosection are indicated by short arrows (C1, C2). *Hoxa13* endodermal expression in the cloaca (CL). (D) expression in the tail and hindlimb bud at St. 22. (E) dissected E4 posterior gut (arrows at endodermal hindgut (HG) and mesodermal cloacal expression), no expression is detected in the ceca (CE) or midgut (MG). (F) protein expression at E6 section of the hindgut in the endoderm (endo) hindgut (arrow).

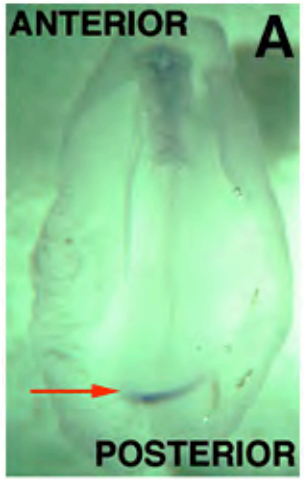
ANTERIOR
A
POSTERIOR

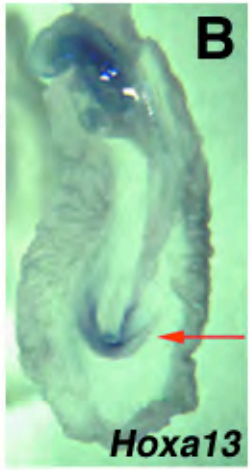
B
Hoxa13

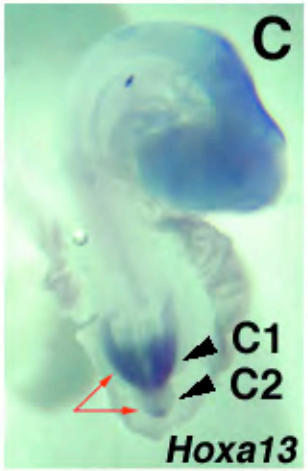
C
C1
C2
Hoxa13

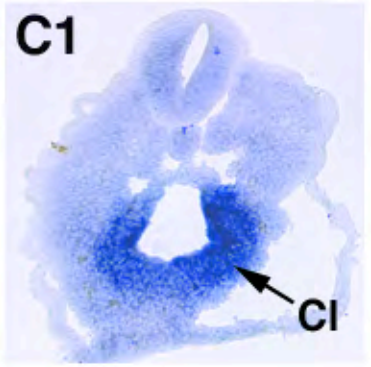
C1
CI

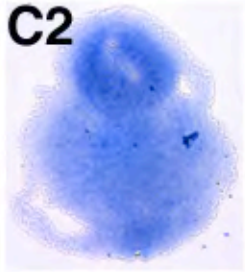
C2

Hoxa13

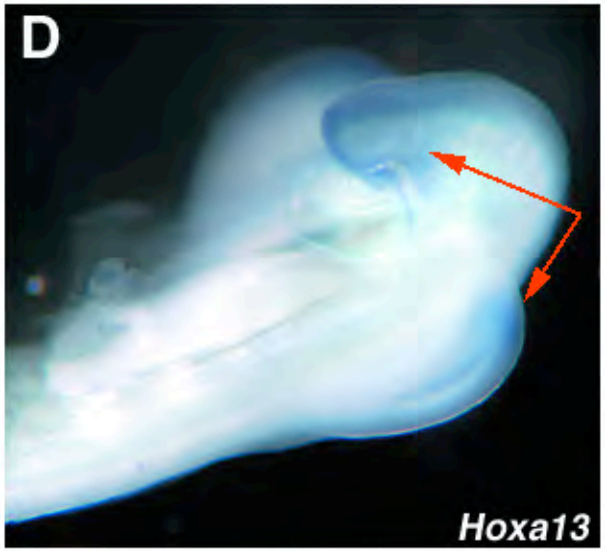
D
Hoxa13

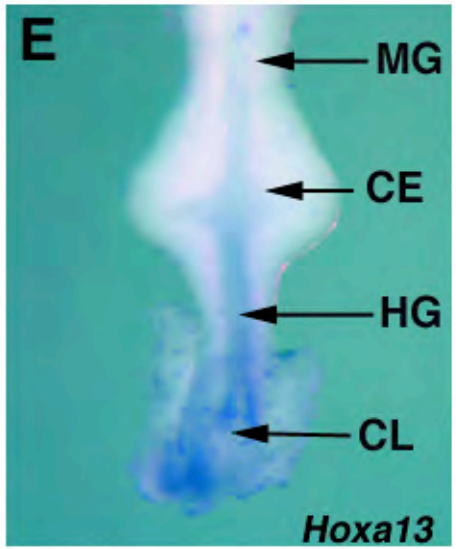
E
MG
CE
HG
CL
Hoxa13


F
endo.
Hoxa13 Ab.

Fig. 2. Human HFG and chick *HFGa13* overexpressed embryos have similar limb phenotypes. (A-D) Control (left panel) and *HFGa13*-infected (right panel) hindlimbs at E6. Planar sections of E6 limbs (B), uninjected control (left) *HFGa13* infected hindlimb (right, arrow shows fibula maldevelopment with undifferentiated mesenchymal cells).(C) In situ hybridization of *Fgf8* in sectioned hindlimb. No *Fgf8* expression is detected in the *HFGa13*-infected hindlimb compare to the uninfected hindlimb (arrows). (D) In situ hybridization of *Bapx1* in sectioned hindlimb. Altered *Bapx1* expression in the *HFGa13*-infected hindlimb (arrows).

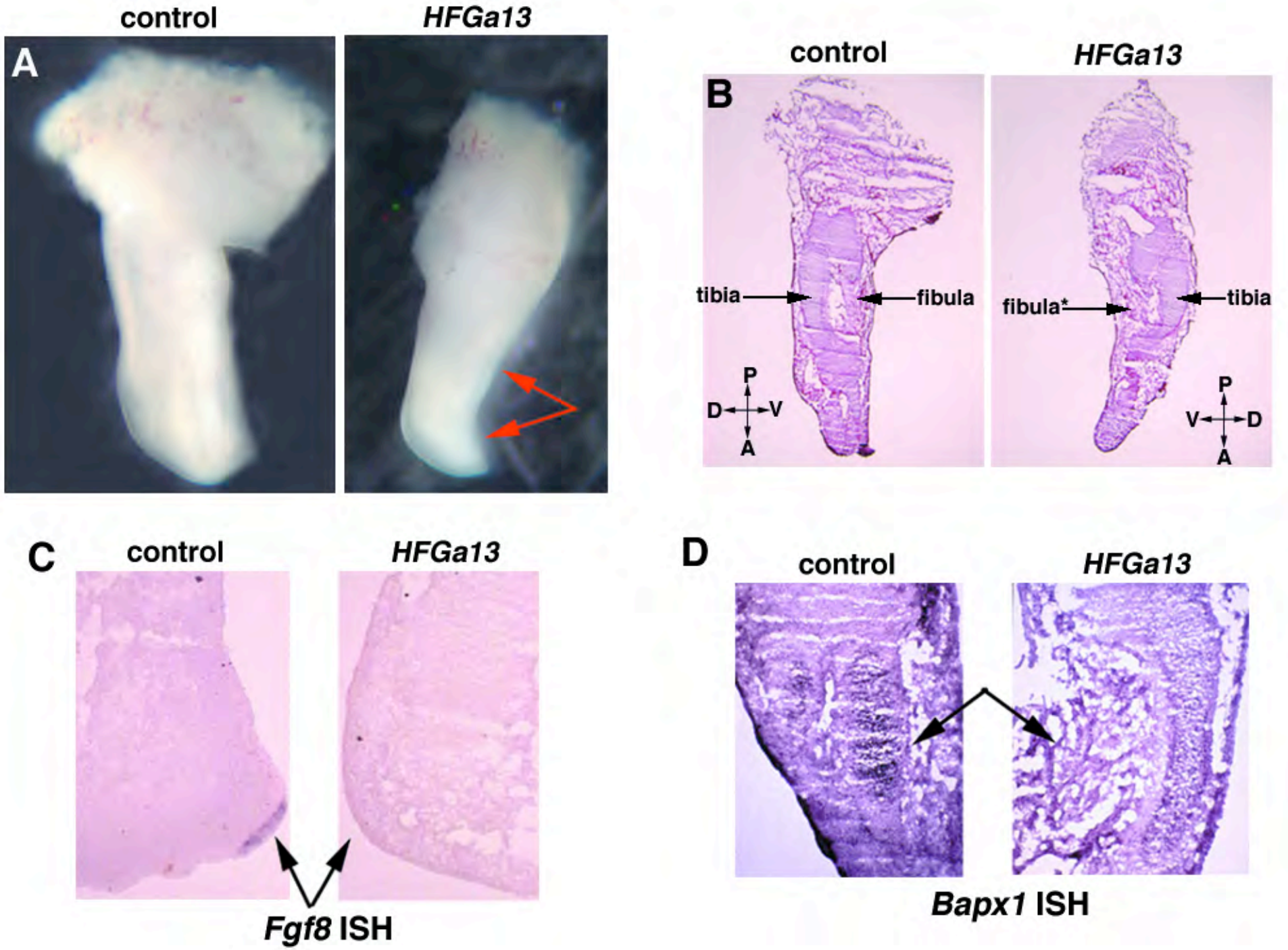
control
HFGa13
A
B
tibia
fibula
fibula*
P
D
V
A
C
Fgf8 ISH
D
Bapx1 ISH

Fig. 3. Endodermally expressed *HFGa13* causes abnormal hindgut and tail development. (A) Whole-mount in situ hybridization showing *RCAS* expression in an E6 mutant *HFGa13* infected embryo. (B) 3C2 immunohistochemistry analysis of sectioned *HFGa13*-infected mutant embryo shows posterior endoderm (endo.) and mesoderm (meso.) infection. (C) *RCAS* in situ showing absence of the mutant phenotype when *HFGa13* infection is present only in the mesoderm, demonstrated in (D) with anti-gag immunohistochemistry showing no infection in the caudal endoderm (E6). (E) E6 survivors after electroporation of *HFGa13* constructs in the posterior endodermal layer. The phenotype involves maldevelopment of the cloaca (CL*), hindgut (HG*), and tail. Allantoic internalization is present (AL*), ceca are unaffected (CE). (F) Anti-Nflag demonstrating expression of the tagged-HFGa13 in the endoderm of the hindgut, mesoderm is not stained. Note the electroporated endodermal cells appear undamaged and intact. Misexpression of *HFGa13* and *Hoxa13* constructs by electroporation show similar expression levels in the gut endoderm layer (data not shown).

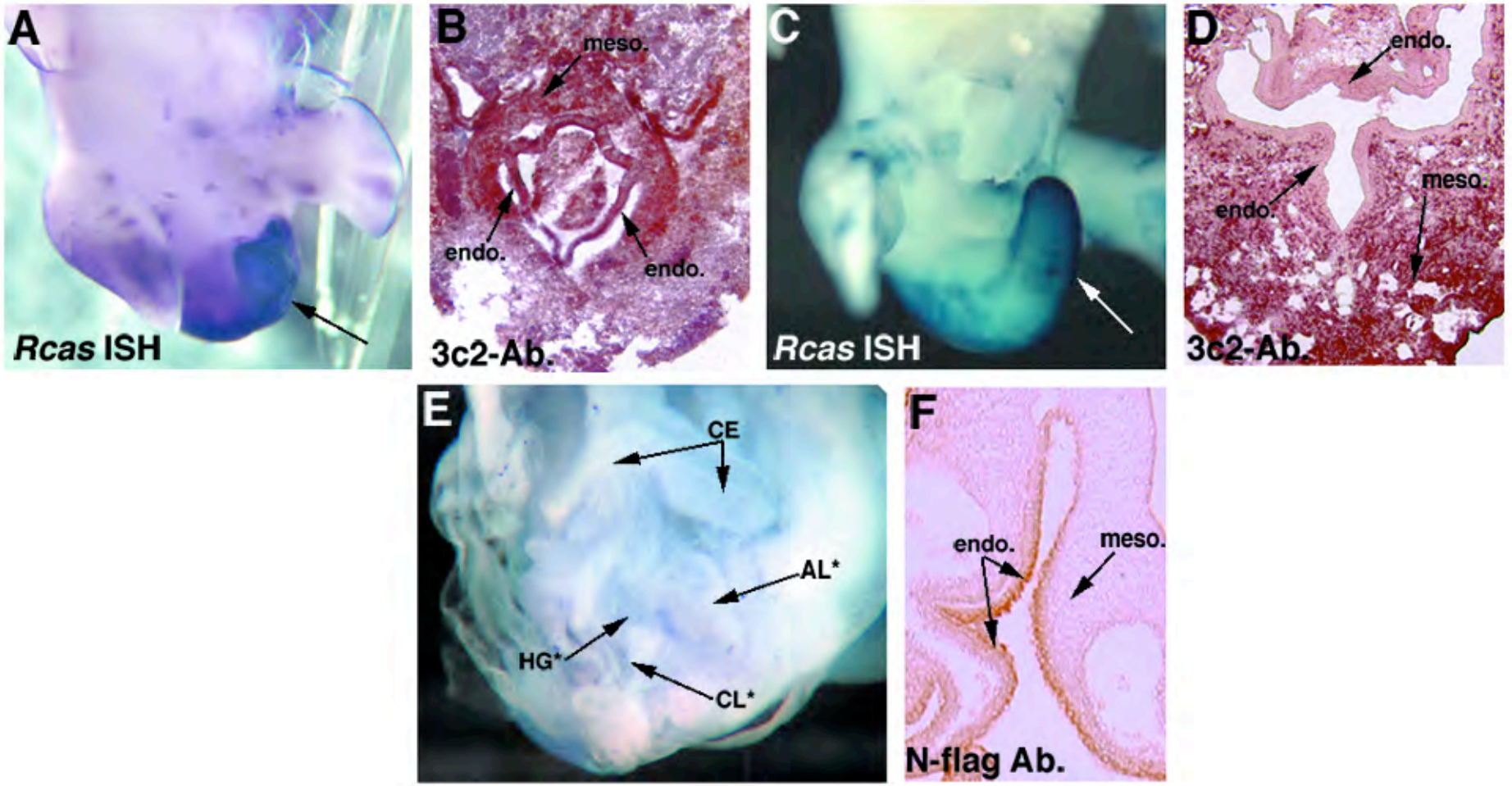
A
Rcas ISH
B
meso.
endo.
endo.
3c2-Ab.
C
Rcas ISH
D
endo.
endo.
meso.
3c2-Ab.
E
CE
AL*
HG*
CL*
F
endo.
meso.
N-flag Ab.

Fig. 4. Histology analysis of mutant *HFGa13*-infected embryos. H&E stained transverse (A-D, E7) and longitudinal (E-H, E6) sections of mutant *HFGa13*-infected (A,C,E,G) and control embryos (B,D,F,H). Ourentery is present in (A). *HFGa13*-infected embryos show cloacal stenosis (C), atresia of the hindgut anterior to the cloaca (E), allantoic internalization (E), and defects in the cloaca-associated viscera including more distal Müllerian duct (MN duct) atresia and cystic mesonephric (MN*) maldevelopment (G). Note the correct development of the more anterior gut structures. Ceca (CE), notochord (NC), other abbreviations as per Fig. 3.

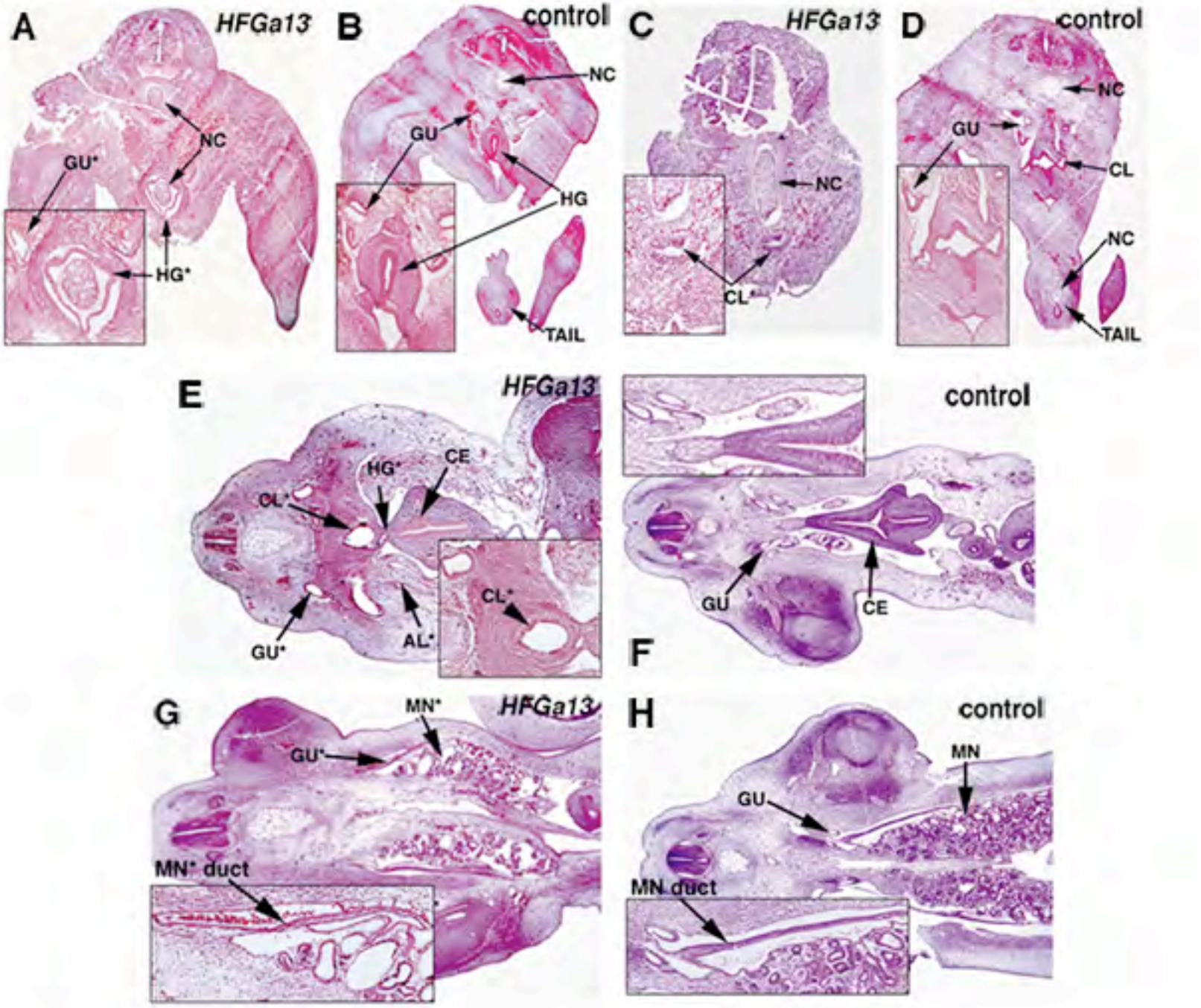
A
HFGa13
NC
GU*
HG*
B
control
NC
GU
HG
TAIL
C
HFGa13
NC
CL*
D
control
NC
GU
CL
NC
TAIL
E
HFGa13
HG*
CE
CL*
CL*
AL*
GU*
F
control
GU
CE
G
HFGa13
MN*
GU*
MN* duct
H
control
MN
GU
MN duct

Fig. 5. *HFGa13* affects expression of *Fgf8*, *Hoxd13* and *Bapx1*. (A-G) Whole-mount in situ hybridizations of control (left panel) and *HFGa13*-infected (right panel) embryos (arrows at malformed tail). (A) *Fgf8* expression at E5, note absence of expression in the HFGa13 tail but normal expression in the hindlimb AER. (B) *Bapx1* (expression) at E6. *Bapx1* shows a diminished expression in the tail of the *HFGa13*-infected embryo, but normal expression in the non-infected hindlimbs. (C) *Wnt5a* gene expression shows expression in the *HFGa13*-infected embryo, E7. (D) *Hoxd13* expression at E6 shows strong down-regulation in the tail *HFGa13*-infected embryo and normal expression in hindlimbs. (E) *Shh* expression at E4 shows is normal. Arrows at hindlimb and notochord.

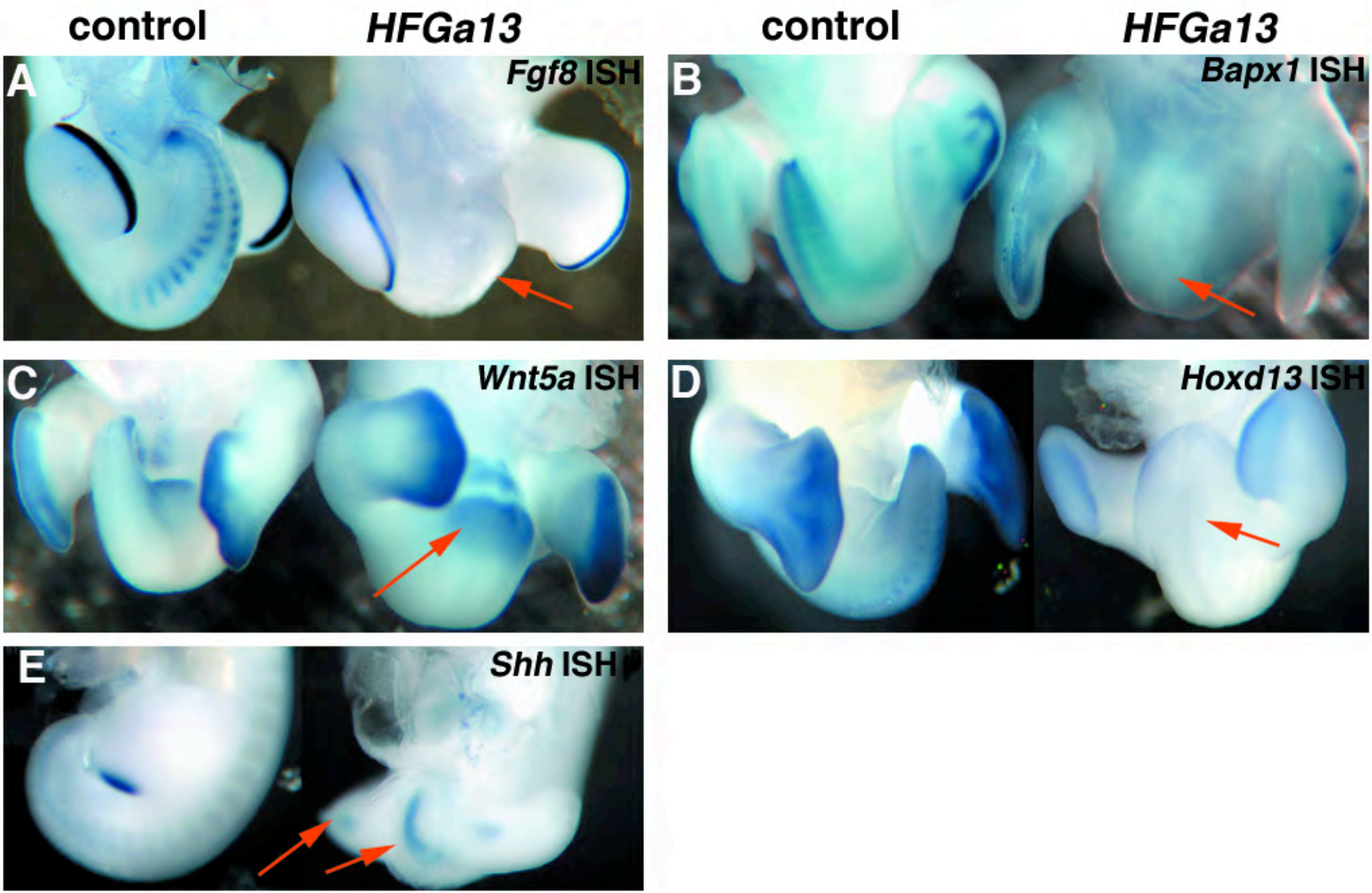
control
HFGa13
control
HFGa13
A
Fgf8 ISH
B
Bapx1 ISH
C
Wnt5a ISH
D
Hoxd13 ISH
E
Shh ISH

Fig. 6. Whole embryo explants developed in culture demonstrate the physical necessity of caudal endoderm for normal tail development. (A) Whole embryo explanted at St. 10 and grown on albumen/agarose for 48 hours showing normal tail development and expression of *Hoxa13* in tail (blue arrow). Arrowhead shows normal placement of allantois ventral to hindgut which expresses *Hoxa13*. (B) St. 10 embryo grown with caudal endoderm removed demonstrating blunted tail without *Hoxa13* expression (long arrow). Short arrow marks hindgut dorsal to *Hoxa13* expressing allantois. (C) H&E section through a caudal endoderm-less embryo that developed ourentery (large arrowhead) within hindgut lumen (short arrow). { shows allantois. Small arrowhead shows normal notochord. (D) Section anterior to (C) showing endoderm (arrows) and notochord (arrowhead). (E) Embryo cultured ~24 hours with caudal endoderm develops normal CIP (long arrow), expresses *Shh* in notochord (red stain, arrowhead, most of notochord deep to plane of photograph), and coexpresses *Shh* and *CdxA* in endoderm of CIP (short arrow, purple/black stain). (F) Embryo cultured ~24 hours without caudal endoderm fails to develop CIP or express *Shh* or *CdxA* in midline caudal endoderm (long arrow), both are coexpressed in right lateral caudal endoderm (short arrow, purple/black stain). Notochord is curved but expresses *Shh* (red stain, arrowhead). (G) Embryo after caudal endoderm removed and donor caudal endoderm transplanted, cultured ~48 hours showing tail growth (long arrow). lb - hindlimb buds. (H) Embryo after caudal endoderm removed and donor anterior endoderm transplanted, cultures ~48 hours showing blunted tail (long arrow), allantois (arrowhead). ht - heart.

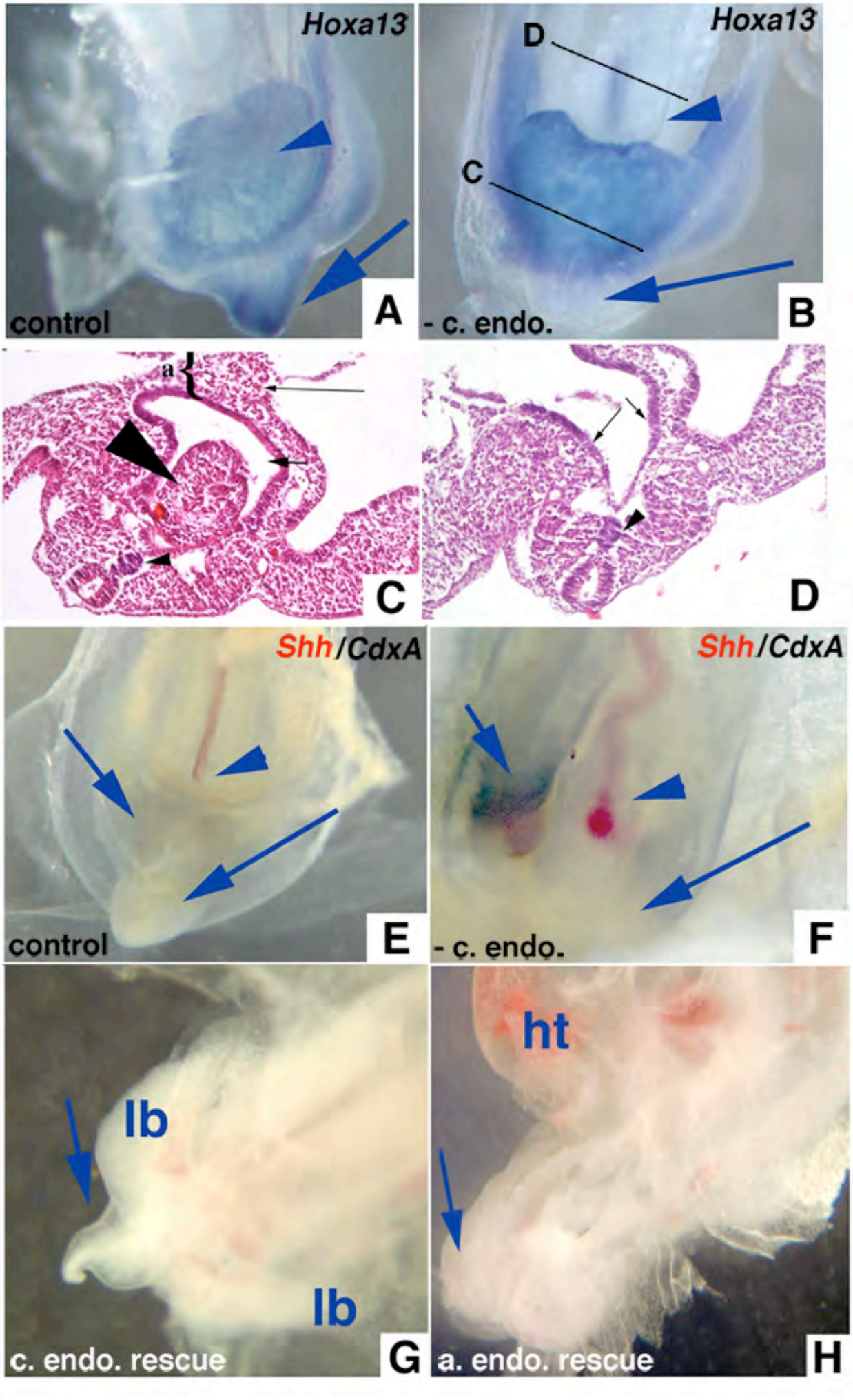
Hoxa13
control
A
Hoxa13
D
C
- c. endo.
B
a
C
D
Shh/CdxA
control
E
Shh/CdxA
- c. endo.
F
lb
lb
c. endo. rescue
G
ht
a. endo. rescue
H

Fig. 7. HFGa13 interferes with the cellular functions of Hoxa13 and Hoxd13.

(A) Transcriptional transactivation by wild-type Hoxa13 and HFGa13 proteins in a GAL4-fusion assay in COS-7 cells. Relative luciferase activities were normalized to the empty GAL4 DNA-binding domain expression vector. Fusion protein of the GAL4 DNA-binding domain and Hoxa13 shows transcriptional activation of the synthetic reporter. In contrast, fusion protein of the GAL4 DNA-binding domain and HFGa13 fails to activate transcription of the same promoter and is able to decrease the basal activity. Luciferase assays were performed after two independent transfections, each done in triplicate (A,B). (B) Perturbation of the transcriptional transactivation of wild-type Hoxa13 and Hoxd13 by HFGa13 in a GAL4-fusion assay in COS-7 cells. In this assay, we monitored GAL4 trasncriptional activity induces by GAL4 DBD fusion proteins without or with pcDNA3-HFGa13 construct. In a same molar ratio, HFGa13 form specifically decreases Hoxa13 and Hoxd13 transcriptional activation. (C, D) Intracellular localization of Hoxa13 and HFGa13 proteins. Immunostaining of transfected N-flag tagged Hoxa13 (C) and HFGa13 (D) constructs in COS-7 cells with specific N-flag antibody show both nuclear localization. Note an additive cytoplasmic signal with the HFGa13 construct. (E-K) H&E sections of E18 control (E,F) or infected (G-K) guts. (E) Normal midgut with thin and long villi. (F) Normal hindgut with flat and short villi. (G) *HFGa13* mesodermally infected midgut has wild-type midgut epithelium. *Hoxa13* (H) and *Hoxd13* (J) mesodermally infected midgut shows hindgut-like epithelial transformation. *HFGa13* co-infected midguts with either *Hoxa13* (I) or *Hoxd13* (K) show rescue of the epithelial hindgut phenotype. (L) *Hoxd13* and *HFGa13* mesodermal midgut co-infection show presence of virus (detected by 3C2-Ab., L1), and ectopic *HFGa13* (detected with

Hoxa13 probe, L2) and *Hoxd13* (L3) co-expressions, associated with normal epithelial phenotype.

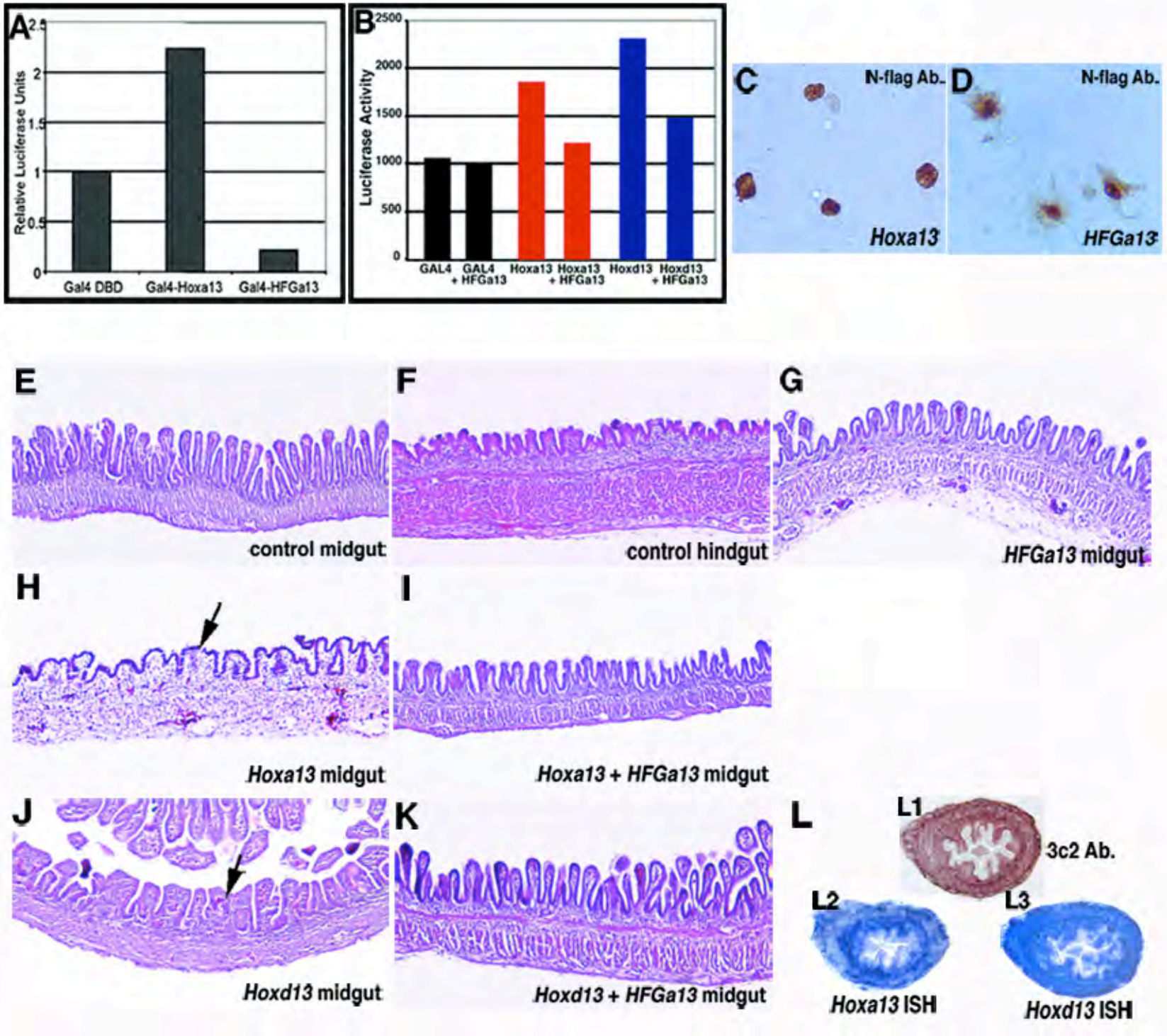
A
Relative Luciferase Units
2.5
2
1.5
1
0.5
0
Gal4 DBD
Gal4-Hoxa13
Gal4-HFGa13
B
Luciferase Activity
2500
2000
1500
1000
500
0
GAL4
GAL4 + HFGa13
Hoxa13
Hoxa13 + HFGa13
Hoxd13
Hoxd13 + HFGa13
C
N-flag Ab.
Hoxa13
D
N-flag Ab.
HFGa13
E
control midgut
F
control hindgut
G
HFGa13 midgut
H
Hoxa13 midgut
I
Hoxa13 + HFGa13 midgut
J
Hoxd13 midgut
K
Hoxd13 + HFGa13 midgut
L
L1
3c2 Ab.
L2
L3
Hoxa13 ISH
Hoxd13 ISH